Sensors and Actuators B 249 (2017) 747–755

Contents lists available at ScienceDirect

Sensors and Actuators B: Chemical

journal homepage: www.elsevier.com/locate/snb

Electrochemical sensor based on molecularly imprinted composite membrane of poly(*o*-aminothiophenol) with gold nanoparticles for sensitive determination of herbicide simazine in environmental samples

Jin Zhang[a,b,*], Chaoying Wang[a], Yanhui Niu[a,b], Shijie Li[b,**], Rongqin Luo[b]

[a] School of Chemistry and Life Science, Guizhou Normal College, Guiyang 550018, PR China
[b] State Key Laboratory of Environmental Geochemistry, Institute of Geochemistry, Chinese Academy of Sciences, Guiyang 550002, PR China

ARTICLE INFO

Article history:
Received 15 October 2015
Received in revised form 24 January 2016
Accepted 16 February 2016
Available online 18 February 2016

Keywords:
Molecular imprinting
Electrochemical sensor
Gold nanoparticles
Herbicide simazine
o-Aminothiophenol

ABSTRACT

A novel electrochemical sensor based on molecularly imprinted polymer membranes (MIPM) as biomimetic molecular recognition element involved in *o*-aminothiophenol functionalized Au nanoparticles (ATP@AuNPs) modified gold electrode was constructed for sensitive and selective detection of herbicide simazine (SMZ). The nano-scaled MIPM, with high specific surface area, was prepared by self-assembly of *o*-aminothiophenol (ATP) and electrodeposition of ATP@AuNPs in the presence of template SMZ. Cathodic current of SMZ was measured by cyclic voltammetry and the results exhibited that the proposed sensor possess a high electrocatalytic activity at a negative potential and a fast rebinding dynamics towards the reduction of SMZ in 0.01 M H_2SO_4 solution (pH 1.7). Linear dependency of peak current on SMZ concentrations was observed from 0.03 to 140 μM and detection limit was estimated to be 0.013 μM (3S/N). The enhancement of sensitivity was attributed to the presence of gold nanoparticles (AuNPs) which decreased the electron-transfer impedance and increased imprinting sites, lead to the superior enrichment effect of the trace amount of SMZ in aqueous solvent. The developed SMZ imprinted sensor exhibited excellent long-term stability and acceptable repeatability. In addition, the proposed method was successfully applied to measure SMZ in several real samples with the spiked recoveries changing from 91.4% to 96.8%, showing a promising potential in practical application.

1. Introduction

Simazine (SMZ,6-chloro-*N*,*N*-diethyl-1,3,5-triazine-2,4-diamine), an usual s-triazine herbicides, is distributed in soil or natural water, and may be spread to adjacent areas due to drift, runoff or evaporation [1]. Serious environmental problems can originate from SMZ persistence due to its low solubility in water and strong sorption on carbonous materials or clays. So SMZ is suspected of being an endocrine disrupting chemical and has potentially hazardous to human health [2]. Several methods such as thin-layer chromatography [3], surface plasmon resonance [4,5], high-performance liquid chromatography [6,7], gas chromatography–mass spectrometry [8] and immunosensor [9,10] have been developed for SMZ quantification. Unfortunately, some of these methods require sophisticated equipment, advanced technical expertise, high cost, and time-consuming. So they are difficult for in situ or online monitoring. Particularly, a biosensor fabricated by using biological receptors is generally expensive and unstable [11]. Consequently, the development of a simple, rapid, inexpensive, stable and sensitive analytical method for routine SMZ screening is of particular significance and necessity.

Molecularly imprinted polymers (MIP), recognized for their versatile adsorption and catalytic properties, is a promising material as the recognition element or modifying agent in the preparation of sensors. MIP has been regarded as good candidate to replace biological receptor and investigated intensively [12,13], owing to their high selectivity, chemical stability, moderate cost and easy preparation [14]. The molecularly imprinted electrochemical sensor (MIECS), however, typically suffers from drawbacks such as poor binding sites resulting in low sensitivity, slow binding kinetics leading to long analysis time, and the reported difficulties related to the integration of the MIP with the transducer [15,16]. To over-

* Corresponding author at: School of Chemistry and Life Science, Guizhou Normal College, Guiyang 550018, PR China. Fax: +86 851 5816647.
** Corresponding author.
E-mail addresses: jzhang@gznc.edu.cn (J. Zhang), lishijie@vip.gyig.ac.cn (S. Li).

http://dx.doi.org/10.1016/j.snb.2016.02.068
0925-4005/

come these situations, electropolymerization with the advantages of simplicity and speed of preparation, thickness and morphology controlling, high reproducibility and the possibility of preparation and operation in aqueous solutions [17,18], is utilized to directly prepare rigid, uniform, and compact MIP films on transducer surfaces [11]. A drawback of electropolymerization is that fewer imprinted sites form on the surfaces of electrode because of the relatively high density of polymers [19], which subsequently decrease the selectivity and sensitivity of MIECS. Fortunately, the nanoparticle-based amplification platforms and amplification processes have been reported to dramatically enhance the intensity of the electrochemical signal and lead to ultrasensitive assays [20]. Thus the integration of various nanoparticles with MIP polymers films have been proposed to overcome the mentioned defects of MIECS [21,22]. In particular, AuNPs have caused considerable interest and been extensively applied in fabrication of MIECS because of their excellent conductivity, good catalytic activity, high effective surface area, easy to be functionalized and quite stable in aqueous environment [23,24].

Previously, we implemented the AuNPs-based amplification platforms to improve the conductivity of MIP films via adsorption of AuNPs to the prepared ATP polymer (PATP) film, which enhanced effectively sensitivity of MIECS and constructed a novel method for indirect detection of tolazoline with ferrocyanide/ferricyanide redox probe [25]. The objectives of this study were (a) to investigate a new design of the MIECS modified by *o*-aminothiophenol functionalized gold nanoparticles (ATP@AuNPs) to prevent from AuNPs aggregation and enhance the immobilized amounts of template per unit surface area, and (b) to apply the as-prepared MIECS for direct and ultrasensitive electrochemical determination of herbicide SMZ in environmental samples using cyclic voltammetry (CV) technique. ATP@AuNPs was prepared firstly as a substrate. Then the electro-polymerization process was implemented on PATP modified gold electrode, in the presence of template molecule SMZ, to form a porous and rigid three-dimensional (3D) SMZ imprinted film. Which contribute to the MIECS exhibited fast rebinding dynamics, high selectivity, excellent sensitivity and prominent stability for ultrasensitive determination of SMZ.

2. Experimental

2.1. Reagents and materials

o-Aminothiophenol (ATP, 99%), *p*-aminobenzenesulfonic acid (ABS) and dodecanethiol (DDE) were purchased from Aladdin Chemistry Co., Ltd. (Shanghai, China). Simazine (SMZ), picloram (PL), acetochlor (AC) and terbutylazine (TL) were obtained from Shanghai Pesticide Research Institute (Shanghai, China). Sodium borohydride ($NaBH_4$) and gold chloride ($HAuCl_4$) were purchased from Sigma Chemical Co. (St. Louis, MO, USA). All chemicals and solvents used were of analytical grade and used as received. Ultrapure water obtained from a Millipore water purification system (≥18 MΩ, Milli-Q, Millipore) was used throughout the experiments. Solutions of either sulfuric acid, for pH < 2, or 0.1 M in both acetic and phosphoric acids, for 2 < pH < 6, were used as supporting electrolytes. The ionic strength was adjusted to 0.3 M with solid NaCl and the pH was adjusted with 0.2 M NaOH. Phosphate buffered solution (PBS, pH 6.8) was prepared using 0.2 M Na_2HPO_4 and 0.2 M KH_2PO_4.

2.2. Apparatus

Electrochemical experiments were carried out with a CHI 660D electrochemistry workstation (Shanghai CH Instruments, China). The AC impedance of the MIP film was measured with the Autolab PGSTAT302 electrochemical analyzer (Metrohm, Switzerland). Scanning Electron Microscope (SEM) images were obtained using a S-4800 Scanning Electron Microscope (Hitachi, Japan). Transmission Electron Microscope (TEM) images were performed on a JEM-2000FX II Transmission Electron Microscope (JEOL, Japan). And Atomic Force Microscope (AFM) images were obtained using a Veeco Introduces Dimension Edge Atomic Force Microscope System (Bruker, USA). All the pH measurements were performed with a MP 230 pH meter (Mettler-Toledo Switzerland).

2.3. Synthesis of the ATP functionalized Au nanoparticles

The ATP@AuNPs was synthesized refering to the method reported elsewhere [26] with slight modifications. Briefly, 10 mL solution containing 197 mg of $HAuCl_4$ in ethanol was added quickly to a 5 mL solution containing 51.1 mg of ABS and 8 mg of ATP in methanol. The mixture solution was stirred in the presence of 2.5 mL of glacial acetic acid in an ice bath for 1 h. Subsequently, 7.5 mL 1.0 M $NaBH_4$ aqueous solution was added dropwise, resulting in a rapid color change from pale yellow to deep red that indicated the formation of AuNPs. The solution was stirred for an additional 1 h in an ice bath and then for 12 h at room temperature (a dark solid confirmed that the AuNPs were coated with ATP). The black solid was separated by centrifuging at a speed of 10000 rpm for 15 min, washed and centrifuged successively (twice in each solvent) with methanol, absolute ethanol and acetone, and then dried in a vacuum oven overnight at 80 °C. The obtained ATP@AuNPs was stored at 4 °C prior to use.

2.4. Fabrication of SMZ imprinted sensor

Prior to modification, gold electrode (Φ = 2 mm) was polished to a mirror-like surface repeatedly by applying 1.0, 0.3 and 0.05 μm alumina slurries on the chamois, respectively. Then it was chemically cleaned by immersing into a freshly prepared mixture of "piranha" solution (a 3:7 mixture of 30% H_2O_2 and conc. sulfuric acid) for 10 min and successively sonicated with ethanol and distilled water for 10 min and then dried in air. Finally the electrode was electropolished via a CV process, with the potential scanning from −0.2 to 1.4 V in 0. 5 M H_2SO_4 until a stable cyclic voltammogram was obtained at 50 mV s^{-1} vs. SCE.

The schematic diagram of the preparation of SMZ imprinted sensor is shown in Scheme 1. Firstly, PATP/Au electrode was prepared by immersing the cleaned electrode for 20 h into deoxygenated 0.01 M H_2SO_4 solution (pH 1.7), with a 20% volume of ethanol solution to ensure the solubility, containing 2 mM ATP and 0.5 mM SMZ. Secondly, PATP/Au electrode was implemented CV scan for 10 cycles in aqueous dispersion of 1.0 mg mL^{-1} ATP@AuNPs and 0.5 mM SMZ under nitrogen atmosphere, at a scan rate of 100 mV s^{-1} between −0.4 V and 0.8 V. Thirdly, the resulting electrode was soaked in 5% DDE ethanol solution for 5 h to seal the blank surface where did not form imprinted PATP film. Finally, the obtained electrode was immersed in 0.01 M H_2SO_4 supporting electrolyte to remove non-polymeric ATP@AuNPs and named as SMZ@MIP/ATP@AuNPs/ATP/Au electrode. As control, non-imprinted polymer modified electrode, was prepared under the same experimental conditions without adding SMZ, both the self-assembly and electrodeposition process, to check the reliability of the measurements.

2.5. SMZ removal from electrode surface

There are electrostatic interactions and hydrogen bonding between ATP monomer and polar groups of SMZ molecules. In order to break the interactions, we used methanol/acetic acid (7:3 v/v) solution in water as a desorption agent. The

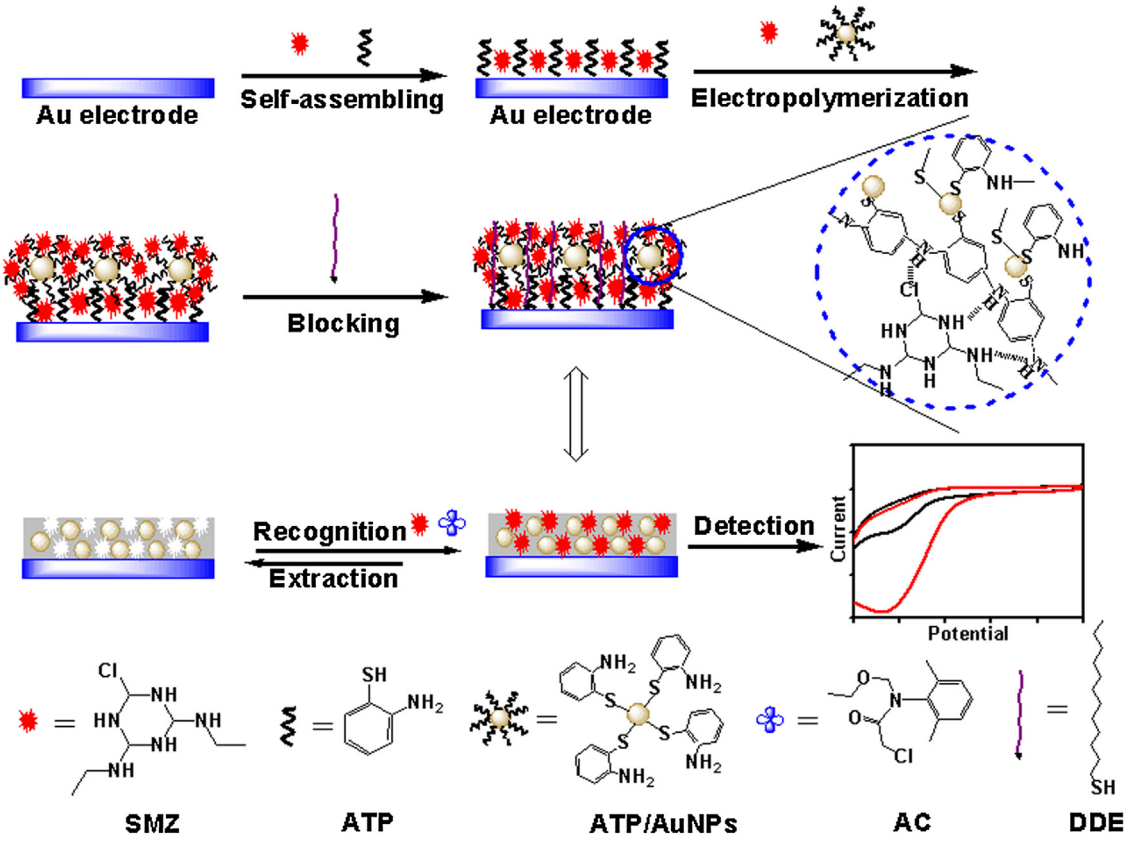

Scheme 1. Schematic representation for the construction process of SMZ imprinted sensor.

completely removal of SMZ was verified electrochemically. SMZ@MIP/ATP@AuNPs/ATP/Au electrode was dipped into 25 mL of desorption agent for 1 h at room temperature under continuous agitation (200 rpm). After SMZ removal, the electrode was washed with ultra-pure quality water and dried under vacuum (200 mmHg, 25 °C), and the obtained electrode, tagged as MIP/ATP@AuNPs/ATP/Au electrode, was stored at 4 °C in dry condition when not in use.

2.6. Electrochemical detection of SMZ

Electrochemical measurements were performed with a conventional three-electrode system composed of the imprinted sensor as working electrode, a saturated calomel electrode (SCE) as reference electrode and platinum wire as auxiliary electrode. The measurements were carried out in a glass vial containing 10 mL deoxygenated electrolyte solution and maintained in nitrogen atmosphere during the experiment at room temperature. The modified process experiments were performed in PBS (pH 6.8) containing 0.1 M KCl and 5.0 mM $[Fe(CN)_6]^{3-/4-}$. The CV potential range was taken from −0.1 to 0.5 V at 50 mV s^{-1}. Electrochemical impedance spectroscopy (EIS) data were measured at 100 kHz~0.1 Hz at wave amplitude of 10 mV and an electrode potential of 0.197 V. Rebinding experiments and selectivity experiments were carried out by immersing the imprinted electrode in a 0.01 M H_2SO_4 solution (pH 1.7) with different SMZ concentrations. After SMZ solution was injected into the vial, the electrodes were incubated for 5 min to ensure SMZ molecule diffuse into the MIP film and rebound by MIP/ATP@AuNPs/ATP/Au electrode, and then washed carefully with distilled water. The data for condition optimization and the calibration curve were the average of three measurements.

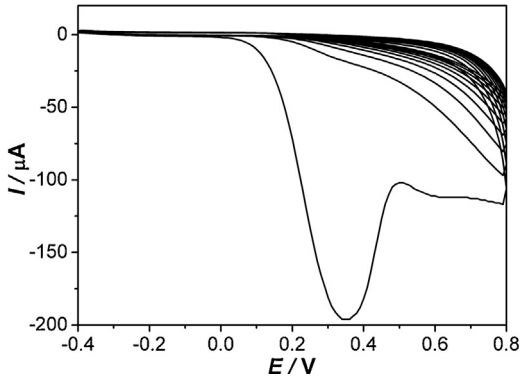

Fig. 1. Repeated cyclic voltammograms for the electrochemical polymerization of ATP@AuNPs in the presence of SMZ in 0.01 M H_2SO_4 solution (pH 1.7) at scan rate of 50 mV s^{-1}.

3. Results and discussion

3.1. The formation of ATP@AuNPs imprinted film

It is a prerequisite for the formation of a strong complex between the template and functional monomer prior to polymerization, and the ATP was chosen for this end. In the self-assembly process, the formed SMZ imprinted ATP monolayer is not only benefit for fixing the MIP film on electrode surface through Au—S covalent bonds between gold electrode and the thiol groups (-SH) of ATP molecules [27,28]. But also serve as an initial polymerizable monolayer to improve the "wetting" of the surface by the polymer [29], which drives the selective occurrence of electrochemical polymerization at the surface of AuNPs. Fig. 1 exhibits a cyclic voltammogram for the modification of ATP@AuNPs onto the monolayer. As shown,

the electropolymerization was an irreversible process. The first sweep showed the characteristic oxidation peak at about 0.35 V and the subsequent scans showed a passivated electrode. The peak current decreased with increasing sweep cycles, indicating that the SMZ imprinted ATP@AuNPs composites film was successfully grafted to the monolayer surface via electrochemical polymerization of the aniline moiety of ATP [20]. During the electrochemical polymerization process, the SMZ molecules diffused towards the surface of ATP@AuNPs and trapped in the PATP@AuNPs matrix owing to ability of these molecules to interact with ATP. SMZ has different functional groups which could be involved in hydrogen-bonding formation with the —NH— group of PATP@AuNPs units. Chain branching and cross linking in PATP@AuNPs generate a 3D matrix with niches containing the template SMZ. The recognition of SMZ molecule is based on shape selection and positioning of the functional groups [30].

3.2. Morphological characterization

The morphology of AuNPs and ATP@AuNPs were analyzed by transmission electron microscopy (TEM). The inset of Fig. 2A displays that the synthesized AuNPs were monodispersed spheres with the smooth surface and a uniformed size of ca. 20 nm. Compared with AuNPs, it is clear that in Fig. 2A the size of the ATP@AuNPs became bigger (the mean size was about 30 nm), darker and their external surface became rough, indicating the ATP was successfully linked on the AuNPs surface. The surface roughness and size distributions of ATP@AuNPs were further measured using atomic force microscopy. As illustrated in Fig. 2B, the AFM image of the ATP@AuNPs exhibited irregular shape in morphology, with sizes of 25–35 nm were homogeneously dispersed, and a rough surface doped some bright spot, verifying the successful synthesis of ATP@AuNPs. The doped AuNPs are expected to enhance electronic transmission rate of PATP film and in turn the ATP might be important for preventing aggregation of AuNPs to maintain high surface area. After electropolymerization, the electrode surface became rather rough and uneven because of the formation of SMZ imprinted ATP@AuNPs composites film (Fig. 2C). This morphology confirms that imprinted film possess a porous and 3D space distribution, the rough surface provides a large surface area for the adsorption of the target species at the modified electrode. Furthermore, after the electrode was continuously immersed in 5% DDE solution for 5 h, the Au electrode surface exhibited a dense coverage with a compact film (Fig. 2D), indicating that DDE can seal the exposed Au surface effectively.

3.3. Electrochemical characteristics

Considering that SMZ has lower electroactivity at the selected working potential range of –0.1 V–0.5 V, $[Fe(CN)_6]^{3-/4-}$ was selected as the probe to evaluate the formation of MIP film on electrode. As illustrated in Fig. 3, well-defined reversible peaks of 5.0 mM $[Fe(CN)_6]^{3-/4-}$ with 106 mV of peak potential difference (ΔE_p) were observed on bare gold electrode (curve a). Only small background response, however, was observed on the SMZ imprinted monolayer film modified electrode (curve b). Compared with the curve b, after covalently rebinding of ATP@AuNPs, the values of ΔE_p decreased significantly (from 106 to 84 mV) with a 13.1 μA increase in the peak current (curve c). This down-shifting demonstrated that the introduction of AuNPs in ATP polymer film played an important role in providing the conducting bridges for the electron transfer of ferrocyanide/ferricyanide couple and increased the effective surface area of electrode, leading to enhanced electron transfer kinetics [24]. After the removal of SMZ, a visible oxidation-reduction peak was observed (curve d). This situation is owing to the removed templates making electronic transfer

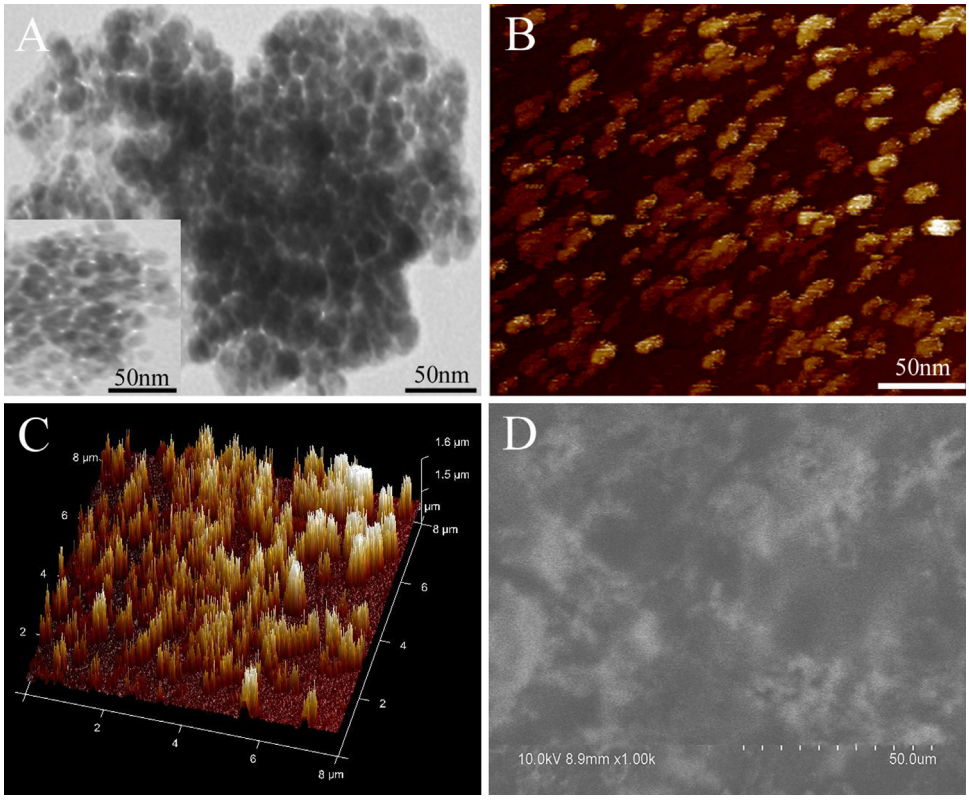

Fig. 2. (A) TEM images of ATP@AuNPs and AuNPs (inset); (B) AFM images of ATP@AuNPs and (C) ATP/Au electrode after electrochemical polymerization of ATP@AuNPs; (D) SEM image of MIP/ATP@AuNPs/ATP/Au electrode after sealing with 1-dodecanethiol.

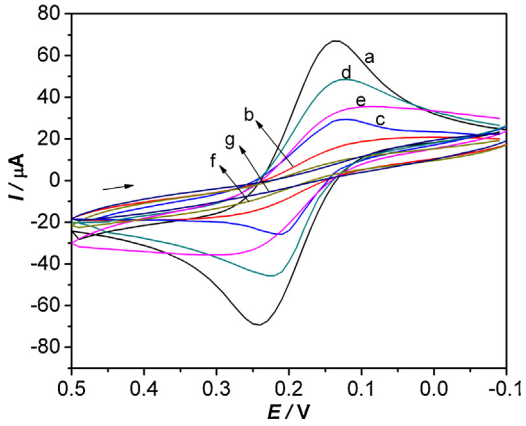

Fig. 3. Cyclic voltammograms of 5.0 mM $[Fe(CN)_6]^{3-/4-}$ in 0.1 M KCl at (a) bare Au electrode, (b) ATP/Au electrode, (c) SMZ@MIP/ATP@AuNPs/ATP/Au electrode, (d) MIP/ATP@AuNPs/ATP/Au electrode and (e) MIP/ATP@AuNPs/ATP/Au electrode after rebinding in 60 μM SMZ, (f) NIP/ATP@AuNPs/ATP/Au electrode before and (g) after undertaking elution process.

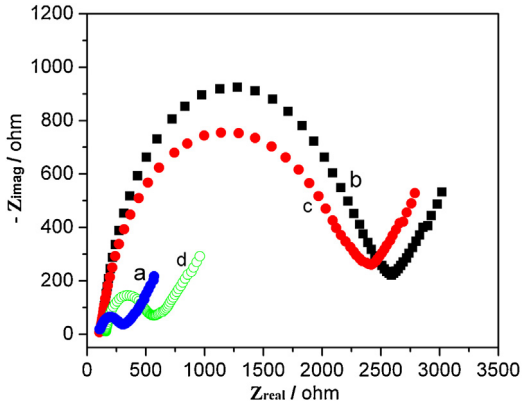

Fig. 4. Electrochemical impedance spectra of (a) bare Au electrode, (b) NIP/ATP@AuNPs/ATP/Au electrode, (c) SMZ@MIP/ATP@AuNPs/ATP/Au electrode (d) MIP/ATP@AuNPs/ATP/Au electrode in 5.0 mM $[Fe(CN)_6]^{3-/4-}$ solution containing 0.1 M KCl.

possible. The peak current from curve d to curve e decreased because the holes of PATP structure were filled. Hence, the electron transfer of $[Fe(CN)_6]^{3-/4-}$ redox couple was blocked again. In contrast, the redox current change of $[Fe(CN)_6]^{3-/4-}$ from curve f to curve g was negligible after the elution step because no cavities formed in non-imprinted polymer (NIP) when the ATP@AuNPs/ATP film polymerized on the electrode in the absence of template SMZ. This finding indicates that the NIP/ATP@AuNPs/ATP/Au electrode was unselective and unrecognizable.

As an effective method for probing the surface features of modified electrode, electrochemical impedance spectroscopy (EIS) was also applied to characterize the stepwise construction process of the SMZ imprinted sensor. The typical impedance spectrum includes a semicircle portion and a linear portion. The semicircle diameter at higher frequencies corresponds to the electron-transfer resistance (R_{et}), and the linear part at lower frequencies corresponds to the diffusion process [31]. As illustrated in Fig. 4, the values of R_{et} were calculated for bare Au electrode, NIP/ATP@AuNPs/ATP/Au electrode, MIP/ATP@AuNPs/ATP/Au electrode before and after elution was 192.8, 2467.5 and 2211.0 and 429.1 Ω, respectively. Curve a displayed almost a straight line in the Nyquist plot, indicating that there was improved diffusion on the bare gold electrode, a big resistance was present in curve b, implying a high electron transfer resistance to the redox-probe and the block of charge transfer by the MIP film formed in

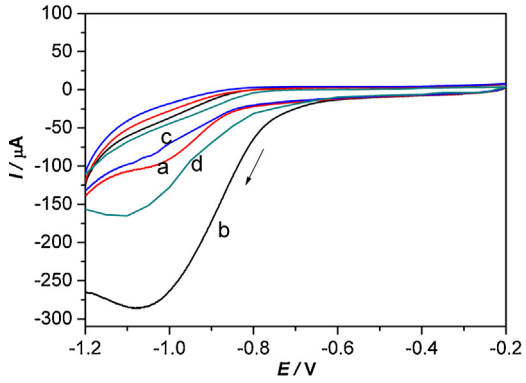

Fig. 5. CV responses of 0.12 mM SMZ in 0.01 M H_2SO_4 solution (pH 1.7) at (a) bare Au electrode, (b) MIP/ATP@AuNPs/ATP/Au electrode, (c) NIP/ATP@AuNPs/ATP/Au electrode and (d) MIP/ATP/Au electrode.

electropolymerization. The R_{et} of MIP/ATP@AuNPs/ATP/Au electrode before (curve c) and after (curve d) extraction of template SMZ possessed larger changes of frequency response, indicating that the template was successfully removed and formed some cavities which facilitated the electron exchange between the redox [32]. In addition, this phenomenon could be attributed to the introduction of AuNPs, which provided more imprinted sites after extraction of template SMZ molecules and in turn left more channels for the penetration of $[Fe(CN)_6]^{3-/4-}$ through the MIP film to the electrode for further oxidation.

3.4. Electrochemical behavior of the proposed sensors

To investigate the electrochemical redox behavior, SMZ was subjected to CV in 0.01 M H_2SO_4 solution (pH 1.7). As seen in Fig. 5, the scanning was started at −0.2 V in the cathodic direction and reversed at −1.20 V. No oxidation signal corresponding to the cathodic response was observed in the anodic branch, indicating the irreversible character of the overall processes. Because of weak catalysis, a poor reduction peak could be observed on the bare gold electrode (curve a). In order to confirm whether the SMZ molecules had been embedded in the MIP/ATP@AuNPs/ATP film, CVs of MIP/ATP@AuNPs/ATP/Au electrodes and NIP/ATP@AuNPs/ATP/Au electrodes were recorded and compared. SMZ exhibits a well-defined reduction peak, correspond to first-order two-electron reduction processes (SMZ suffers a cleavage of the Cl atom to yield a dechlorinated intermediate) [33], at −1.09 V was observed at the MIP/ATP@AuNPs/ATP/Au electrode (curve b), but no peak for the NIP/ATP@AuNPs/ATP/Au electrode (curve c), indicating the successful fabrication of imprinted cavities and it is feasible to use ATP@AuNPs to prepare electropolymers with highly catalytic ability towards the reduction of SMZ. To be specific, the peak on MIP/ATP@AuNPs/ATP/Au electrode was 23 times more than bare gold electrode, 56 times more than NIP/ATP@AuNPs/ATP/Au electrode and about 10 times more than MIP/ATP/Au electrode (curve d). The higher reduction current verified that AuNPs as an enhancer played an important role in the preparation of MIP film, due to their high adsorption capacity for the template, increased surface area and good conductivity. Additionally, the creation of the molecular imprints is favored by the diffusion of the electroactive template, generating a far higher number of recognition sites during the electrodeposition of the polymer, which result in a large amount of SMZ was concentrated in the MIP layer on the gold electrode from the solution [34].

3.5. Optimal conditions for the electrochemical detection

In this study, AuNPs were used to immobilize the functional monomer ATP to form a rigid 3D framework structure via S—Au bond, which can in turn prevent from AuNPs aggregation and enhance the immobilized amounts of template per unit surface area. Thus, the concentration of the ATP@AuNPs was an important parameter that affected the sensitivity and selectivity of the sensor for SMZ recognition. Three electrodes were electropolymerized in ATP@AuNPs concentrations of 0.5, 1.0 and 2.0 mg mL^{-1}, with a constant SMZ concentration of 0.5 mM. As illustrated in Fig. 6A, the current response reached maximum with the concentration of 1.0 mg mL^{-1}, and then decreased with further increasing of ATP@AuNPs concentration. A lower peak current at ATP@AuNPs concentration lower than 1.0 mg mL^{-1} may be due to the less capture of SMZ during electropolymerization. However, the decrease in current response when the concentration of ATP@AuNPs was above 1.0 mg mL^{-1} could be resulted from template molecules situated at the central area of the polymer membranes cannot completely be removed from polymer matrix [30]. Thus, the optimum concentration of ATP@AuNPs for preparing MIECS was 1.0 mg mL^{-1}.

The thickness of the imprinted film is another important factor affecting the recognition ability of imprinted sensor and it could easily be adjusted by controlling the number of CV scanning cycles during the electropolymerization process. To investigate the effect of CV scanning cycles on the electrochemical response of SMZ, the imprinted sensor was prepared with constant ATP@AuNPs concentration of 1.0 mg mL^{-1} and varying CV scanning cycles in the range of 2–18 cycles. As shown in Fig. 6B, it was found that the maximum peak current was obtained for 10 potential cycles, and then decreased with further increasing the scanning cycles. Although greater deposition of ATP@AuNPs contributes to a higher number of imprinted sites and better membrane stability, it becomes difficult to remove the template from excessively thick membranes. This reduces the number of accessible imprinted sites, leading to low binding capacity and slow kinetics [35,36]. Thus, 10 potential cycles was chosen for the electrochemical polymerization to obtain the highest sensitivity for the determination of SMZ.

In order to illustrate the efficiency of prepared SMZ imprinted electrode, the adsorption dynamics experiment was carried out by recording the current response of MIP/ATP@AuNPs/ATP/Au electrode in 60 μM SMZ solution for different time. As shown in Fig. 6C, the peak current of MIP/ATP@AuNPs/ATP/Au electrode increased sharply with the incubation time up to 3 min and then leveled off slowly, indicating the rapid recognition ability of the imprinted film and its high affinity to the target molecule. Longer incubation time did not obviously improve the response. As a result, a time of 3 min incubation is taken as compromise for all the experiments. The improved sensitivity and speedy balance response were ascribed to the introduction of ATP@AuNPs, which decreased electric resistance of the MIECS and accelerated the immobilization of SMZ to the MIECS. The integration of nanoparticles in MIP materials has the benefits of enhancing the number of accessible complementary cavities, the catalytic activity of the surface and the fast equilibration with the analyte [37]. This electrochemical advantage will allow real-time analysis of SMZ in spot specimens, thereby representing a novel approach for rapid assessment.

The effect of working buffer pH on the MIP/ATP@AuNPs/ATP/Au electrode was also studied by measuring the SMZ concentrations of 60 μM, in pH range 0.5–5.0. The dependence of the peak currents on pH is shown in Fig. 6D. As can be noticed that the reduction peak current has biggish (and roughly pH-independent) values below ca. pH 2.0, and the maximum response at about 1.7, then decreased sharply with pH increases further. As we known, SMZ has a pK (aqueous) value of the ring nitrogen N5 of 1.7 [33], which implies that above this pH value the protonated form of the compound predominates in the solution. The experimental result also indicates that protons play a role in the electrochemical reaction of SMZ on the MIP/ATP@AuNPs/ATP/Au electrode and protons participated in the catalytic reaction. When the solution pH is 1.7, the interaction between SMZ and the PATP film is facilitated. And above this pH, the protonated SMZ interacts weakly with the functional groups of

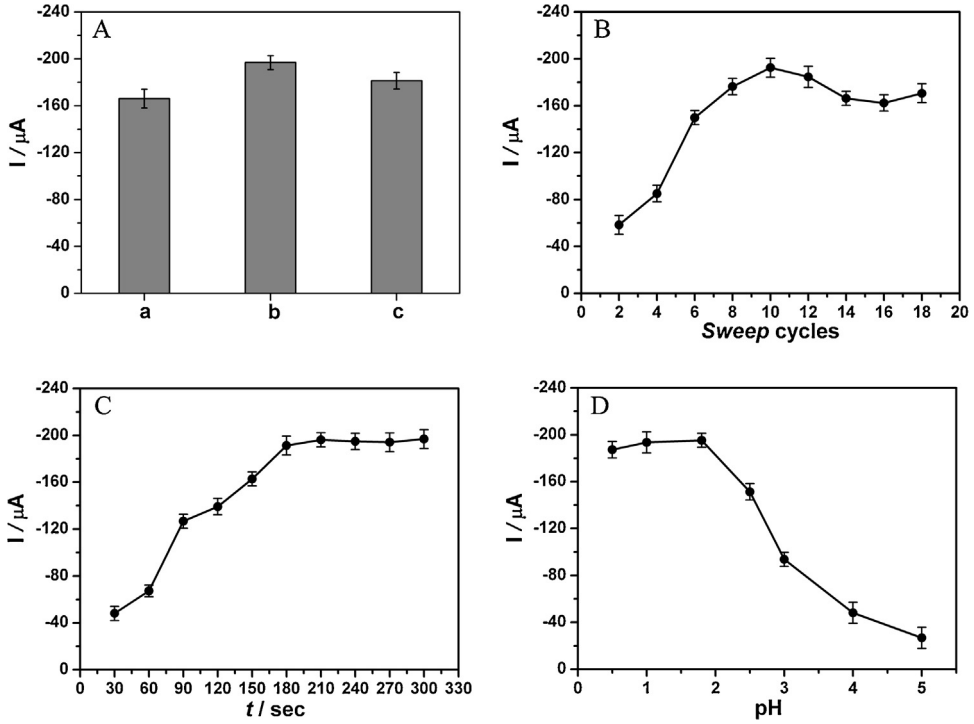

Fig. 6. Effects of (A) ATP@AuNPs concentration, (a) 0.5, (b) 1.0 and (c) 2.0 mg mL^{-1}; (B) sweep cycles; (C) incubation time and (D) extermal solution pH on the amperometric response of 60 μM SMZ on MIP/ATP@AuNPs/ATP/Au electrode.

the recognition site [33]. Thus, pH 1.7 was selected as the optimum pH and used in the remaining experiments.

3.6. Performance of the SMZ imprinted sensor

3.6.1. CV response and calibration curve

A series of river water samples with varying SMZ concentrations were measured under the optimal experimental conditions to determine the calibration curve of the developed sensors. The relation between the cathodic peak current and the SMZ concentration was illustrated in Fig. 7. The good relationship was observed at the SMZ concentration range from 0.03 to 140 μM, described by a mathematical expression $i(\mu A) = -1.491[SMZ](\mu M) - 104.33$, with a correlation coefficient of 0.99 ($n = 3$) and a relative standard deviation (RSD) lower than 3.1%. The detection limit, estimated as the SMZ concentration yielding an amperometric signal equal to three times the peak-to-peak noise of the baseline, was estimated to be 0.013 μM, which was much lower than 0.4 μM for a SMZ MIP sensing based on gold chip [34]. The sensor presented more sensitive response could be owe to the AuNPs, which have an important role in the matrix, for the enhancement of the conductivity by increasing the electron transfer, and for the number of imprinted sites, leading to abundant and homogenous distribution of the recognition sites [38]. Moreover, the sensitivity of AuNPs properties, such as color, surface plasmon resonance, electrical conductivity and binding affinity is significantly enhanced when AuNPs are subjected to functionalize with appropriate metals, organic or biomolecular functional groups [39]. So it was demonstrated that the electrochemical detection of SMZ became more sensitive with the usage of ATP@AuNPs composites as the reduced substrate. As a result, the MIP receptor layer can enrich the trace amount of SMZ from sample solution and made it contact to the surface of the gold electrode.

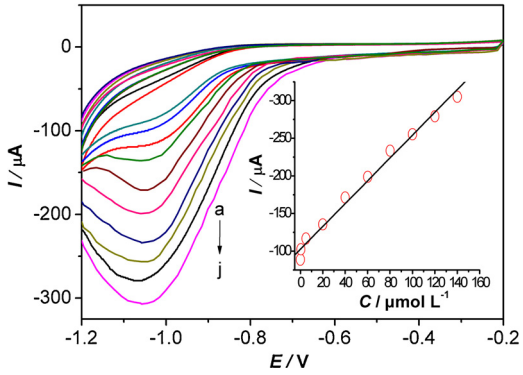

Fig. 7. CV curves for SMZ detection using the proposed sensor in 0.01 M pH 1.7 H_2SO_4 solution containing 0.03, 0.3, 3, 20, 40, 60, 80, 100, 120 and 140 μM SMZ (from a to j). Inset: Plot of peak current vs. SMZ concentration.

3.6.2. Affinity and selectivity of the imprinted sensor

Selectivity is one of potential merits for MIECS. To substantiate the selectivity, competitive transport studies were undertaken. Three possible coexisting electroactive components and analogous structures, picloram (PL), acetochlor (AC) and terbutylazine (TL), were chosen to evaluate the specific recognition ability of the prepared sensor. CV responses of SMZ, TL, AC and PL with individual concentrations of 2, 20, 60, 100 and 140 μM on MIP/ATP@AuNPs/ATP/Au electrode were compared and the results are shown in Fig. 8A. Notably, the MIP modified electrode exhibited a much higher current response toward SMZ than that of the structural analogues. No perceivable difference of current response, however, was observed for any of these analogues, showing that MIP film had the highest specific selectivity toward SMZ. Furthermore, the anti-interference property of the sensor was evaluated via calculating the cathode peak current ratio (I_m/I_o) of CV response in the presence of structural analogs. I_m and I_o were cathode peak current of SMZ at −1.09 V in the presence and absence of interferences, respectively [40]. As seen from Fig. 8B, compared with reference peak current ratio of SMZ ($I_m/I_o = 1$), I_m/I_o was only slightly changed from 91.7% to 106.1% in 20-fold excess of interfering substances. The origin of selective recognition can be attributed to the size and arrangement of functional group of specific cavities matched with SMZ in the MIP/ATP@AuNPs/ATP film created by the imprinting process. Therefore, these results demonstrated that the imprinted sensor can avoid the interference of the coexisting electroactive components existed commonly in environmental samples and thus can allow the detection of SMZ in a complex matrix without separation.

3.6.3. Regeneration and long-term storage stability of the imprinted sensor

The reproducibility of the SMZ imprinted sensor was investigated by measuring the CV responses of 2 μM SMZ at the same electrode following retention/removal processes. The RSD for 30 successive detections is about 3.5%, indicating acceptable fabrication reproducibility. MIP/ATP@AuNPs/ATP/Au electrode was stored at 4 °C under desiccated condition when not in use and measured intermittently (every 2 days). The CV peak current response decreased to 95.2% of its original current after the first 10 days storage period, and was approximately 90.5% of its original response after 30-day period. The RSD of peak current was calculated to be 4.1% for five successive washing and determination operations, indicating the favorable long-term storage stability of the proposed sensor in this experiment, which could be attributed to the rigid

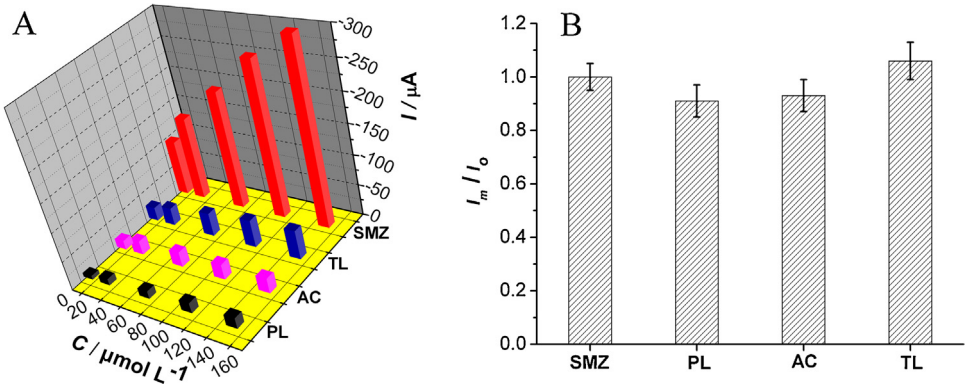

Fig. 8. (A) MIP/ATP@AuNPs/ATP/Au electrode response for different concentrations of SMZ, TL, AC and PL, respectively; (B) Peak current ratio (I_m/I_o) of MIP/ATP@AuNPs/ATP/Au electrode to 60 μM SMZ and 60 μM SMZ in the presence of 1.2 mM PL, AC, and TL, respectively.

Table 1
Results for the determination of SMZ in local water and soil samples.

Environmental samples	Added (μM)	Founded[a] (μM)	Recovery% (mean ± SD, $n = 5$)
Tap water	2	1.91	95.6 (±1.4)
	40	38.71	96.8 (±2.1)
River water	2	1.86	93.2 (±2.2)
	40	38.09	95.2 (±1.9)
Soil	2	1.83	91.4 (±2.6)
	40	37.64	94.1 (±1.7)

[a] The results were expressed as mean value based on five replicates.

3D framework structure arises from the ATP@AuNPs that involves Au—S bonds and hydrogen–bond interaction between the template and monomer, lead to a reversible complexation and exchange between SMZ and recognition sites in the MIP film.

3.7. Preliminary analysis of real samples

In an attempt to evaluate the feasibility of the proposed method for practical applications, MIP/ATP@AuNPs/ATP/Au electrode was applied to detect SMZ by CV in several environmental samples, including tap water, river water, and soil samples (collected from Guiyang, China) under optimized conditions. Prior to analysis, freshly collected water samples (obtained from Nanming River, Guiyang, China) were immediately filtered through a millipore cellulose nitrate membrane (pore size was 0.45 μm) to remove suspended particles. The collected wet soil was dried in air and extracted with absolute ethanol for 1 h. After centrifugation filtration, the filtrate was collected and diluted to mark with 0.01 M H_2SO_4. Then the pH of all samples was adjusted to 1.7. As no SMZ was found in all samples, the standard addition method was adopted and the results are summarized in Table 1. The recoveries of the proposed method were in the range from 91.4% to 96.8% and the alteration of RSD was below 2.88%, suggesting an acceptable deletion result. Therefore, the developed imprinted sensor could be reliable and effective for the determination of SMZ in the real sample matrix.

4. Conclusions

In the present paper, a simple and sensitive monitoring method of SMZ was proposed by stepwise fabricating of PATP film and a thin MIP/ATP@AuNPs film on gold electrode. From the preceding results, we have demonstrated that ATP@AuNPs could effectively prevent from AuNPs aggregation via forming a rigid 3D framework structure, enhance electron transport and increase the immobilized amounts of template per unit surface area, which leads to prominent improvement of the selectivity and sensitivity of SMZ imprinted sensor. The detection limit was 0.012 μM and the the peak on MIP/ATP@AuNPs/ATP/Au electrode was 23 times more than bare gold electrode or 56 times more than NIP/ATP@AuNPs/ATP/Au electrode. In addition, SMZ was detected selectively more than structurally-similar herbicides, such as AC, TL and PL, without the matrix interference of environmental sample. In summary, the proposed sensor provided a simple and reliable technique for SMZ detection in environmental samples and a notion to perfect the MIP-based sensor for trace detection.

Acknowledgements

This work was supported by the Science-Technology Foundation of Guizhou Province (Grant No. J20152125), the Provincial Department of Education Foundation of Guizhou Province (Grant No. 2014321), State Key Laboratory of analytical chemistry for life science Foundation of Nanjing University (Grant No. SKLACLSS1417), the Foundation of guizhou education university (Grant No. 20154).

References

[1] M.T. Strandberg, J.J. Scott-Fordsmand, Field effects of simazine at lower trophic levels—a review, Sci. Total Environ. 296 (2002) 117–137.
[2] J. Kniewald, M. Jakominić, A. Tomljenović, B. Šimić, P. Romac, Đ. Vranešić, Z. Kniewald, Disorders of male rat reproductive tract under the influence of atrazine, J. Appl. Toxicol. 20 (2000) 61–68.
[3] J. Sherma, N.T. Miller, Quantitation of the triazine herbicides atrazine and simazine in water by thin layer chromatography with densitometry, J. Liq. Chromatogr. 6 (1980) 901–910.
[4] C. Mouvet, R.D. Harris, C. Maciag, B.J. Luff, J.S. Wilkinson, J. Piehler, A. Brecht, G. Gauglitz, R. Abuknesha, G. Ismail, Determination of simazine in water samples by waveguide surface plasmon resonance, Anal. Chim. Acta 338 (1997) 109–117.
[5] R.D. Harris, B.J. Luff, J.S. Wilkinson, J. Piehler, A. Brecht, G. Gauglitz, R.A. Abuknesh, Integrated optical surface plasmon resonance immunoprobe for simazine detection, Biosens. Bioelectron. 14 (1999) 377–386.
[6] H. Katsumata, A. Fujii, S. Kaneco, T. Suzuki, K. Ohta, Determination of simazine in water samples by HPLC after preconcentration with diatomaceous earth, Talanta 65 (2005) 129–134.
[7] O.L. de Sabando, Z.G. de Balugera, M.A. Goicolea, E. Rodríguez, M.C. Sampedro, R.J. Barrio, Determination of simazine and cymoxanil in soils by microwave-assisted solvent extraction and HPLC with reductive amperometrical detection, Chromatographia 55 (2002) 667–671.
[8] W.T. Ma, Z. Cai, G.B. Jiang, Determination of atrazine, deethylatrazine and simazine in water at parts- per- trillion levels using solid- phase extraction and gas chromatography/ion trap mass spectrometry, Rapid Commun. Mass Spectrom. 17 (2003) 2707–2712.
[9] M.F. Yulaev, R.A. Sitdikov, N.M. Dmitrieva, E.V. Yazynina, A.V. Zherdev, B.B. Dzantiev, Development of a potentiometric immunosensor for herbicide simazine and its application for food testing, Sens. Actuators B: Chem. 75 (2001) 129–135.
[10] N.F. Starodub, B.B. Dzantiev, V.M. Starodub, A.V. Zherdev, Immunosensor for the determination of the herbicide simazine based on an ion-selective field-effect transistor, Anal. Chim. Acta 424 (2000) 37–43.
[11] P.S. Sharma, A. Pietrzyk-Le, F.D. Souza, W. Kutner, Electrochemically synthesized polymers in molecular imprinting for chemical sensing, Anal. Bioanal. Chem. 402 (2012) 3177–3204.
[12] S.A. Piletsky, E.V. Piletskaya, A.V. Elgersma, K. Yano, I. Karube, Y.P. Parhometz, A.V. El'skaya, Atrazine sensing by molecularly imprinted membranes, Biosens. Bioelectron. 10 (1995) 959–964.
[13] R. Shoji, T. Takeuchi, I. Kubo, Atrazine sensors based on molecularly imprinted polymer- modified gold electrode, Anal. Chem. 75 (2003) 4882–4886.
[14] A. Ramanaviciene, A. Finkelsteinas, A. Ramanavicius, Basic electrochemistry meets nanotechnology: electrochemical preparation of artificial receptors based on a nanostructured conducting polymer, polypyrrole, J. Chem. Educ. 83 (2006) 1212–1214.
[15] X.L. Xu, G.L. Zhou, H.X. Li, Q. Liu, S. Zhang, J.L. Kong, A novel molecularly imprinted sensor for selectively probing imipramine created on ITO electrodes modified by Au nanoparticles, Talanta 78 (2009) 26–32.
[16] J. Zhang, Y.H. Niu, S.J. Li, R.Q. Luo, C.Y. Wang, A molecularly imprinted electrochemical sensor based on sol–gel technology and multiwalled carbon nanotubes—Nafion functional layer for determination of 2-nonylphenol in environmental samples, Sens. Actuators B: Chem. 193 (2014) 844–850.
[17] B. Rezaei, M.K. Boroujeni, A.A. Ensa, A novel electrochemical nanocomposite imprinted sensor for the determination of lorazepam based on modified polypyrrole@sol–gel@gold nanoparticles/pencil graphite electrode, Electrochim. Acta 123 (2014) 332–339.
[18] A.C. Roy, V.S. Nisha, C. Dhand, M.A. Ali, B.D. Malhotra, Molecularly imprinted polyaniline-polyvinyl sulphonic acid composite based sensor for para-nitrophenol detection, Anal. Chim. Acta 777 (2013) 63–71.
[19] C. Xue, Q. Han, Y. Wang, J. Wu, T. Wen, R. Wang, J. Hong, X. Zhou, H. Jiang, Amperometric detection of dopamine in human serumby electrochemical sensor based on gold nanoparticles doped molecularly imprinted polymers, Biosens. Bioelectron. 49 (2013) 199–203.
[20] M.L. Yola, T. Eren, N. Atar, Molecularly imprinted electrochemical biosensor based on Fe@ Au nanoparticles involved in 2-aminoethanethiol functionalized multi-walled carbon nanotubes for sensitive determination of cefexime in human plasma, Biosens. Bioelectron. 60 (2014) 277–285.
[21] W.J. Lian, S. Liu, J.H. Yu, X.R. Xing, J. Li, M. Cui, J.D. Huang, Electrochemical sensor based on gold nanoparticles fabricated molecularly imprinted polymer film at chitosan–platinum nanoparticles/graphene–gold nanoparticles double nanocomposites modified electrode for detection of erythromycin, Biosens. Bioelectron. 38 (2012) 163–169.
[22] C. Xue, X. Wang, W.Y. Zhu, Q. Han, C.H. Zhu, J.L. Hong, X.M. Zhou, H.J. Jiang, Electrochemical serotonin sensing interface based on double-layered membrane of reduced graphene oxide/polyaniline nanocomposites and molecularly imprinted polymers embedded with gold nanoparticles, Sens. Actuators B: Chem. 196 (2014) 57–63.
[23] V.K. Shukla, P. Yadav, R.S. Yadav, P. Mishra, A.C. Pandey, A new class of PANI-Ag core–shell nanorods with sensing dimensions, Nanoscale 4 (2012) 3886–3893.

[24] P.T. Do, P.Q. Do, H.B. Nguyen, V.C. Nguyen, D.L. Tran, T.H. Le, L.H. Nguyen, H.V. Pham, T.L. Nguyen, Q.H. Tran, A highly sensitive electrode modified with graphene, gold nanoparticles, and molecularly imprinted over-oxidized polypyrrole for electrochemical determination of dopamine, J. Mol. Liq. 198 (2014) 307–312.
[25] J. Zhang, Y.Q. Wang, R.H. Lv, L. Xu, Electrochemical tolazoline sensor based on gold nanoparticles and imprinted poly-*o*-aminothiophenol film, Electrochim. Acta 55 (2010) 4039–4044.
[26] M. Riskin, Y. Ben-Amram, R. Tel-Vered, V. Chegel, J. Almog, I. Willner, Molecularly imprinted au nanoparticles composites on au surfaces for the surface plasmon resonance detection of pentaerythritol tetranitrate, nitroglycerin, and ethylene glycol dinitrate, Anal. Chem. 83 (2011) 3082–3088.
[27] M. Riskin, R. Tel-Vered, T. Bourenko, E. Granot, I. Willner, Imprinting of molecular recognition sites through electropolymerization of functionalized au nanoparticles: development of an electrochemical TNT sensor based on π–donor–acceptor interactions, J. Am. Chem. Soc. 130 (2008) 9726–9733.
[28] Z.F. Huang, F. Chen, P.A. Bennett, N.J. Tao, Single molecule junctions formed via Au-thiol contact: stability and breakdown mechanism, J. Am. Chem. Soc. 129 (2007) 13225–13231.
[29] E. Sabatani, Y. Gafni, I. Rubinstein, Morphology control in electrochemically grown conducting polymer films. 3. A comparative study of polyaniline films on bare gold and on gold pretreated with *p*-aminothiophenol, J. Phys. Chem. 99 (1995) 12305–12311.
[30] A.E. Radi, A.E. El-Naggar, H.M. Nassef, Molecularly imprinted polymer based electrochemical sensor for the determination of the anthelmintic drug oxfendazole, J. Electroanal. Chem. 729 (2014) 135–141.
[31] L. Alfonta, E. Katz, I. Willner, Sensing of acetylcholine by a tricomponent-enzyme layered electrode using faradaic impedance spectroscopy, cyclic voltammetry, and microgravimetric quartz crystal microbalance transduction methods, Anal. Chem. 72 (2000) 927–935.
[32] X. Li, X. Wang, L. Li, H. Duan, C. Luo, Electrochemical sensor based on magnetic graphene oxide@ gold nanoparticles-molecular imprinted polymers for determination of dibutyl phthalate, Talanta 131 (2015) 354–360.
[33] M.J. Higuera, M. Ruiz Montoya, R. Marín Galvín, J.M. Rodríguez Mellado, A contribution to the study of the electroreduction of 2-chloro-4,6-di(ethylamino)-1,3,5-triazine(simazine) on mercury electrodes, J. Electroanal. Chem. 474 (1999) 174–181.
[34] Y. Fuchiwaki, R. Shoji, I. Kubo, H. Suzuki, 6-Chloro-*N*,*N*-diethyl-1,3,5-triazine-2,4-diamine(simazine) electrochemical sensing chip based on biomimetic recognition utilizing a molecularly imprinted polymer layer on a gold chip, Anal. Lett. 41 (2008) 1398–1407.
[35] C. Xie, B. Liu, Z. Wang, D. Gao, G. Guan, Z. Zhang, Molecular imprinting at walls of silica nanotubes for TNT recognition, Anal. Chem. 80 (2008) 437–443.
[36] L.J. Kong, M.F. Pan, G.Z. Fang, X.L. He, Y.K. Yang, J. Dai, S. Wang, Molecularly imprinted quartz crystal microbalance sensor based on poly(*o*-aminothiophenol) membrane and Au nanoparticles for ractopamine determination, Biosens. Bioelectron. 51 (2014) 286–292.
[37] S. Tokonami, H. Shiigi, T. Nagaoka, Review: micro-and nanosized molecularly imprinted polymers for high-throughput analytical applications, Anal. Chim. Acta 641 (2009) 7–13.
[38] S. Pramanik, C. Zheng, X. Zhang, T.J. Emge, J. Li, New microporous metal-organic framework demonstrating unique selectivity for the detection of high explosives and aromatic compounds, J. Am. Chem. Soc. 133 (2011) 4153–4155.
[39] V.K. Upadhyayula, Functionalized gold nanoparticle supported sensory mechanisms applied in detection of chemical and biological threat agents: a review, Anal. Chim. Acta 715 (2012) 1–18.
[40] Y.K. Yang, G.Z. Fang, G.Y. Liu, M.F. Pan, X.M. Wang, L.J. Kong, X.L. He, S. Wang, Electrochemical sensor based on molecularly imprinted polymer film via sol–gel technology and multi-walled carbon nanotubes-chitosan functional layer for sensitive determination of quinoxaline-2-carboxylic acid, Biosens. Bioelectron. 47 (2013) 475–481.

Biographies

Jin Zhang obtained his M.S. in 2010 from Southwest University, China. He is professor at School of Chemistry and Life Science, Guizhou Normal College. Currently he is a Ph.D. candidate in Chinese Academy of Sciences. His major research interests include electrochemical sensors and environmental analytical chemistry.

Chao-Ying Wang is a professor of analytical chemistry at School of Chemistry and Life Science, Guizhou Normal College. Her research focuses on molecular spectroscopy, electroanalytical chemistry and environmental analytical chemistry.

Yan-Hui Niu obtained her M.S. in 2008 from Shanxi Normal University, China. She is an associate professor at School of Chemistry and Life Science, Guizhou Normal College. Her research interest is electrochemical sensors.

Shi-Jie Li is a professor at Institute of Geochemistry, Chinese Academy of Sciences. He obtained his Ph.D. in 1993 from Chinese Academy of Sciences. His research focuses on Lake Sediment and Environmental Analysis.

Rong-Qin Luo is Ph.D. candidate in Chinese Academy of Sciences. Her major research interest is environmental analytical chemistry.